

On the Use of MATLAB to Import and Manipulate Geographic Data: A Tool for Landslide Susceptibility Assessment

Michele Placido Antonio Gatto ¹, Salvatore Misiano ^{1,*} and Lorella Montrasio ²

¹ Department of Engineering and Architecture, University of Parma, 43121 Parma, Italy; micheleplacidoantonio.gatto@unipr.it

² Department of Civil, Environmental, Architectural Engineering and Mathematics, University of Brescia, 25121 Brescia, Italy; lorella.montrasio@unibs.it

* Correspondence: salvatore.misiano@unipr.it

Abstract: Most of the methods for landslide susceptibility assessment are based on mathematical relationships established between factors responsible for the triggering of the phenomenon, named the conditioning factors. These are usually derived from geographic data commonly handled through Geographical Information System (GIS) technology. According to the adopted methodology, after an initial phase conducted on the GIS platform, data need to be transferred to specific software, e.g., MATLAB, for analysis and elaboration. GIS-based risk management platforms are thus sometimes hybrid, requiring relatively complex adaptive procedures before exchanging data among different environments. This paper describes how MATLAB can be used to derive the most common landslide conditioning factors, by managing the geographic data in their typical formats: raster, vector or point data. Specifically, it is discussed how to build matrices of parameters, needed to assess susceptibility, by using grid cell mapping units, and mapping them bypassing GIS. An application of these preliminary operations to a study area affected by shallow landslides in the past is shown; results show how geodata can be managed as easily as in GIS, as well as being displayed in a fashionable way too. Moreover, it is discussed how raster resolution affects the processing time. The paper sets the future development of MATLAB as a fully implemented platform for landslide susceptibility, based on any available methods.

Keywords: landslide susceptibility assessment; MATLAB Mapping Toolbox; GIS; landslide conditioning factors



Citation: Gatto, M.P.A.; Misiano, S.; Montrasio, L. On the Use of MATLAB to Import and Manipulate Geographic Data: A Tool for Landslide Susceptibility Assessment. *Geographies* **2022**, *2*, 341–353. <https://doi.org/10.3390/geographies2020022>

Academic Editors: Elzbieta Bielecka, Małgorzata Luc and Daniel Moya

Received: 9 May 2022

Accepted: 9 June 2022

Published: 11 June 2022

Publisher's Note: MDPI stays neutral with regard to jurisdictional claims in published maps and institutional affiliations.



Copyright: © 2022 by the authors. Licensee MDPI, Basel, Switzerland. This article is an open access article distributed under the terms and conditions of the Creative Commons Attribution (CC BY) license (<https://creativecommons.org/licenses/by/4.0/>).

1. Introduction

Landslides are high-risk natural phenomena, which occur typically in mountain areas with different mechanisms: slide, flow, fall [1]; they are widespread all over the world, representing a severe threat, due to the landscape damage and loss of human lives that they cause. Haque et al. [2] reported 11,698 injuries and 163,658 deaths due to more than 3876 landslides that occurred between 1995 and 2014 in 128 countries around the world. There is therefore a need to protect territories from landslides; authorities and decision makers manage landslide risk with land planning and risk mitigation strategies, often including monitoring and warning systems. Preliminary to risk management is the assessment, prediction, and mapping of landslide susceptibility.

Methodologies for the assessment of landslide susceptibility can be classified into qualitative and quantitative, both of which aim to define the susceptibility as low, moderate, or high. Qualitative techniques rely on the experience and judgement of experts and are based on the analysis of quasi-static variables; they are considered subjective [3]. Quantitative techniques rationalise the process, carrying out a numerical evaluation through different methodologies, all united by the analysis of factors responsible for triggering the phenomenon, named “conditioning factors”; they usually include lithology, aspect,

and land use [4]. These factors are analysed in light of several techniques, grouped into statistical, such as bivariate (Frequency Ratio or Weight of Evidence) and multivariate (Logistic Regression or Discriminant method) [5–11], or deterministic, such as empirical or physically based [12–19]. Recently, methods based on Artificial Intelligence (AI), and specifically Machine Learning, are wide-spread; examples of Machine Learning techniques are Artificial Neural Networks, the Kernel-based Support Vector Machine (SVM), Tree-based decision trees, or Fuzzy Clustering [20–32].

Conditioning factors are derived from geographical data (geodata); their dissemination in digital format has been favoured thanks to Geographical Information System (GIS) technology. GIS is a milestone in environmental management for natural hazards, disasters, and global climate change; it allows management of geodata, even big volumes, and displays them spatially. Geoprocessing functions available in several GIS-based software, like ArcGIS, also allow the application of several statistical quantitative techniques described above for landslide susceptibility evaluation [31]; however, for the application of physically based models or the use of AI, most previous research shows the realisation of hybrid platforms, which are often very complex. Montrasio et al. [15,16] elaborated GIS-derived geodata in MATLAB for the application of the SLIP Model, i.e., a model for the prediction of rain-induced shallow landslides, on a regional scale; a similar approach was employed by Gutiérrez-Martín [18]. MATLAB was used by Kamran et al. [26] to implement several SVM kernel functions, and by Arnone et al. [21], who employed a specific tool for Neural Networks; both provided MATLAB with ArcGIS-derived geodata. After elaborating the geodata through MATLAB, the landslide susceptibility map is then visualised in a GIS environment. To the authors' knowledge, there is a lack of studies entirely conducted in MATLAB, even for the geodata import. This would allow us to avoid some technical problems regarding compatibility [22].

This article shows how to use MATLAB and disregard the GIS environment to handle geodata; this is the starting point for the realisation of more efficient fully implemented MATLAB platforms in landslide risk management, based on any quantitative technique for landslide susceptibility mapping. Section 2 describes the numerical procedures to import raster, shapefile and point data, directly in a MATLAB environment and assign them to a reference grid cell. Section 3 shows the application of the procedures to derive some of the conditioning factors in a study area affected by landslides during the past. Finally, Section 4 presents a discussion and a comparison of the time required by each procedure varying the spatial resolution of the reference grid.

2. Materials and Methods

Landslide susceptibility assessment and mapping (LSM) require a preliminary and suitable selection of the mapping unit, defined as a homogeneous portion of land surface, which affects the accuracy of the susceptibility evaluation itself. Different methods have been proposed for the landscape division: grid cells, terrain units, unique condition units, slope units and topographic units [33–39]; due to the matrix, the most common is the grid unit form, as it is efficient for data storage and computer implementation [40]. Since MATLAB is one of the best mathematical software to manage matrix data, the grid unit form is selected as a reference in this article. In the following, the technical procedure is described to import geodata containing or referring to some of the most-used conditioning factors for LSM: digital terrain model, lithology, land use and rainfalls. Geodata are provided in a different format (raster, vector or point data), each of them requiring a specific import procedure; then, data matrices are derived by assigning the conditioning parameters to the same spatial grid, named reference grid. Even in this case, different procedures are used according to the geodata format. Most of the mathematical functions discussed in the following require the MATLAB Mapping Toolbox.

2.1. Digital Terrain Model (Raster File)

The Digital Terrain Model (DTM) represents the starting point to build the reference grid; it is provided as georeferenced Raster files that MATLAB may read in several formats: “Tagged Image File + Tif World File” (.tif + .tfw), “GeoTIFF” (.tif), or “ASCII” (.asc). The specific functions to be applied in each format case are summarised in Table 1; outputs of this procedure are the elevation matrix E (row number n , column number m) and an array R , defined as MapCellsReference; the latter is articulated in fields, including: information about the DTM extension (XWorldLimits, YWorldLimits), resolution (CellExtentInWorldX, CellExtentInWorldY), number of points (RasterSize) and the Coordinate Reference System (CRS; ProjectedCRS and GeographicCRS). Generally, for large areas of interest it may be necessary to read different rasters, which the area is divided into, through a for-loop. Each raster is stored in a specific position of a *cell* array. *cell* is a variable class which allows the storage of heterogeneous data, both in terms of element number and type. Thus, even if a study area is included between different projected reference systems, geodata are stored with their own reference systems separately.

Table 1. Summary of the functions used for importing DTM of several formats.

Format	Function
.tif + .tfw	$E = \text{imread}(' .tif')$ $R = \text{worldfileread}(' .tfw', 'planar', \text{size}(E))$
.tif (GeoTiff)	$[E, R] = \text{readgeoraster}(' .tif/.asc', 'OutputType',$
.asc	$'double')$

The coordinates of the reference grid (stored in matrices X and Y) are computed as:

$$[X, Y] = \text{worldGrid}(R) \quad (1)$$

where R is the MapCellsReference array.

Elevation is not the only “conditioning factor” derivable from the DTM; other morphologic factors, commonly computed from the DTM, can be the slope angle β or the aspect angle α [4,26,27,29]. MATLAB allows the computation of them through a function called *3gradient*; this requires the elevation matrix E and the GeographicCellsReference R_1 :

$$[\alpha, \beta, \delta N, \delta E] = \text{gradientm}(E, R_1) \quad (2)$$

where δN and δE are, respectively, the north and eastern gradient. If the DTM is provided in Cartographic coordinates, R_1 is derivable after having converted the reference grid into geographic coordinates through the function *projinv*:

$$[yLat, xLong] = \text{projinv}(R.\text{ProjectedCRS}, X, Y) \quad (3)$$

where $xLong$ and $yLat$ are the geographic coordinate matrices, which have the same structure of X and Y . *LatMin*, *LatMax*, *LongMin* and *LongMax* are the map limits in geographic coordinates; R_1 , required by Equation (2), is obtained through function *georefcells*:

$$R_1 = \text{georefcells}([LatMin, LatMax], [LongMin, LongMax], \text{size}(E)) \quad (4)$$

Sometimes, raster data are provided only through the Open Geospatial Consortium (OGC) and its services of Web Map (WMS) and Web Coverage (WCS). MATLAB allows downloads from WMS (as long as the related *UrlMap* is known), by means of the functions *WebMapServer*, *wmsinfo* and *wmsread*, obtaining the E matrix and the R array. Equation (5) shows an example of code lines for this purpose; map limits and cell size are specified.

```

ServerMap = WebMapServer(UrlMap);
info = wmsinfo(UrlMap);
orthoLayer = info.Layer(1);
[E, R] = wmsread(orthoLayer, 'LatLim', [LatMin,LatMax], 'LonLim',[LongMin,LongMax], 'CellSize','CellExtent');

```

(5)

2.2. Lithology and Land Use Import (Shapefile)

Lithology and land use are considered as “landslide susceptibility factors” by different authors [29,32]: lithology indirectly provides information about soil type, whose mechanical behaviour directly governs the slope failure mechanism; information regarding land use is generally useful to detect anthropised (and altered) areas, as well as to define the risk level based on distance criteria (e.g., distance from roads or residential areas). Lithology and land use are reported here together, because they are commonly provided as “categorical data”, i.e., fields classified according to specific categories (or attributes), including in polygon form. The typical distribution format of their geodata is a Shapefile.

MATLAB reads Shapefiles (.shp) with the function *shaperead*; note that a specific ‘BoundingBox’ can be selected, and if the file is in Latitude–Longitude coordinates ‘UseGeoCoords’ equal to ‘true’ can be specified. *Shaperead* returns a *structure* array (*ReadShape*) containing fields in the rows and attributes in the columns; one of the most important attributes for the geospatial positioning of the polygons are the vertex coordinates (stored in *ReadShape.X* and *ReadShape.Y*). As a first step, the function *shapeinfo* is useful (its output of structure type is referred to as *InfoShape*); it summarises some information as the ‘ShapeType’, ‘BoundingBox’, ‘Attributes’ or ‘CoordinateReferenceSystem’. The latter is fundamental in order to make all the conditioning factors consistent in terms of reference system. To simplify the management of this data type, we suggest deriving a polygon for each field and storing them in a *polyshape* array. Assuming a shapefile in projected coordinates with just one field, the following code lines may be followed, consisting of coordinate conversion and polygon creation:

$$[VertexLat, VertexLon] = projinv(InfoShape.CoordinateReferenceSystem, cat(2,ReadShape.X), cat(2,ReadShape.Y)) \quad (6a)$$

$$FieldPolygon = polyshape([VertexLat, VertexLon]', 'Simplify', false) \quad (6b)$$

Sometimes, fields may be made up of disjoint polygons, i.e., a group of several polygons located in different positions; MATLAB treats this case with a “NaN-approach”: the vertex coordinates of these polygons are contained in a unique column and the NaN (Not a Number) value is placed at the end of each series of coordinates belonging to a single polygon.

Matrices of conditioning factors must also be consistent in terms of discretisation (resolution). As mentioned above, the present article considers the grid cell as the mapping unit and all the conditioning factors are referred to a reference grid. the information on lithology and land use being contained in polygons, a “polygon-raster” conversion is performed. The importance of this conversion is remarked upon by Arnone et al. (2016), who show the use of some built-in ArcGIS options. The original procedure proposed here is based on the solution through MATLAB to a classical geometrical problem of “point-in-polygon” [41]. In other words, it is established which field polygon includes each of the reference grid points. The function used for this purpose is *inpoly* [42]; note that to avoid wrong solutions of the point-in-polygon problem, polygons must be converted from “NaN” to “node-edge” format. This is possible thanks to the function *getnan2* [43]:

$$[nodes, edges] = getnan2(FieldPolygon.Vertices) \quad (7a)$$

$$in = inpoly([xLong,yLat], nodes, edges) \quad (7b)$$

where *in* is a Boolean logic array with 1 located in the position of points that are inside the polygon, otherwise 0. *xLong* and *yLat* contain the reference grid geographic coordinates, as discussed in Section 2.1. This approach allows us to assign specific soil parameters (mechanical and hydraulic) to the reference grid, depending on the polygon of lithology, which includes each point. By applying the variable *in* as index of *xLong* and *yLat*, it is therefore possible to extrapolate geographic coordinates of points inside a specific polygon and generate other conditioning factors. The mechanical and hydraulic properties of soil can be related to different lithologies, according to simple associations [15]. In such a way, the conditioning factors of soil can be created, e.g., cohesion, friction angle or permeability:

$$\text{Cohesion}(in) = c_value \quad (8a)$$

$$\text{Friction}(in) = fi_value \quad (8b)$$

$$\text{Permeability}(in) = k_value \quad (8c)$$

where *c_value*, *fi_value* and *k_value* are scalar variables, readable from Excel files or tables containing the abovementioned association.

2.3. Rainfall (Point Data)

Rainfall is a conditioning factor in the susceptibility analysis of rain-induced shallow landslides [15,16,26,27,29]. Generally, rainfall data refer to past or future events, through rain gauge recordings or predictions of climatic models, respectively. In the first case, rain measurements are provided as “point data”, i.e., data referred to points of known coordinates (gauging stations); they are stored in Excel or Ascii files, importable to MATLAB through the *readcell* function. In the second case, climatic models return the predictions assigned to a grid, included in grib files; for their import, a specific toolbox *nctoolbox* is required [44]. In both cases, rain data need to be distributed to the reference grid, through an interpolation procedure. Several methods have been shown in the literature to spatially distribute a few data points to a large area: Thiessen polygon, Isohyetal, average arithmetic, Krigin and inverse distance weight (IDW) [10,45]. In MATLAB, this can be done through the *scatteredInterpolant* function, suitable to interpolate both irregular and regular scattered data; this function allows the use of three interpolation methods: linear, nearest neighbour or natural neighbour interpolation, which you can choose by specifying, respectively, ‘linear’, ‘nearest’ or ‘natural’ among the input of the function; the latter is used in the present article. By applying the function to the coordinate arrays of the scattered points (*xLongSta*, *yLatSta*) and the array of the recording/prediction rainfall data referred to each of them (*RainData*), the interpolant function *F* is computed:

$$F = \text{scatteredInterpolant}(xLongSta, yLatSta, RainData, 'natural') \quad (9)$$

Input array arguments must be in column form. *F* is then applied to the reference grid coordinate matrices to obtain the interpolated rainfall matrix *h_w*:

$$h_w = \max(0, F(xLong, yLat)) \quad (10)$$

With the code reported in Equation (10), negative values are excluded because they have no physical meaning. To avoid saving irrelevant information (i.e., zero values) for the landslide susceptibility assessment, data can be stored in *sparse* matrices. Note that *h_w* refers to the interpolation of a single rain episode; if a temporal analysis must be performed with a rainfall time history, this procedure must be repeated for each rainfall event.

2.4. Other Useful Operations

In the following, it is described how some useful operations, common to the GIS environment, may be handled even in MATLAB.

2.4.1. Geoprocessing Procedures

Among the common GIS-geoprocessing procedures, merging, clipping, and raster resampling (specifically, resolution downscaling) are of relevance.

The merging procedure is useful to manage high-resolution DTM (or raster, more generally); to avoid a big file size, a regional DTM is often divided into a set of DTMs of smaller extension. To cover a specific study area, it may be required to manage a certain number of DTM files together; this can be done by storing each DTM matrix in a different position of a *cell* array. Note that, similarly, a 3D-matrix-based approach may be used, by saving each DTM in a different third-dimension position; however, this approach can be adopted only when all DTMs to be stored have the same raster size, i.e., the same number of rows or columns. For a generic procedure, the cell-based one is preferred.

The clipping procedure allows us to focus susceptibility analyses on a specific study area, including inside certain territorial limits (municipality, province, region). Limits are usually contained in Shapefile and treated as polygons, as indicated in Section 2.2. It is then possible to clip both a raster and a categorical vector. In the first case, the *inpoly* function is used (see Section 2.2); this allows us to define the index of the grid matrix included in the study area polygon. Clipping a vector is instead possible through the application of the *intersect* function to two polygons (or a set of polygons).

The choice of the most suitable raster resolution for a landslide susceptibility analysis has been discussed by several authors [21]. The resampling of raster data and their downscaling may be essential to improve the computational efficiency of a susceptibility analysis. Thanks to the matrix form of raster data, resampling by downscaling is easily managed by selecting from the original matrix row and column elements with a certain step, according to the integer value of the ratio new/original resolution. In this way, a reduced matrix is obtained.

2.4.2. Geometric Measurement

It could be of interest to measure the extent of a certain area, e.g., the study area or a zone belonging to a specific category. Since areas are managed as polygons, their extent is returned by the function *polyarea*. A conditioning factor that can be derived from geometric measurement is the “distance from roads”. Roads are generally stored in Shapefile geodata. A specific function that can be applied for computing the distance of each point of the reference grid from roads is *p_poly_dist* [46].

2.4.3. User-Defined Parameter Classification

A preliminary procedure when performing a landslide susceptibility assessment consists in grouping some conditioning factors in classes, according to specific numeric value ranges. From a conditioning factor matrix, it is possible to select the index of points whose value is included in a specific interval, by using the *find* function. As an example, to select the index *Ind* of the *E* matrix where the elevation ranges between values *a* and *b*, the following code line can be used:

$$Ind = find(E \leq b \ \& \ E \geq a) \quad (11)$$

3. The Conditioning Factors for a Landslide Susceptibility Assessment of Enna Municipality (Sicily, Italy)

The procedures described in Section 2 are now applied to a study area, which includes Enna Municipality (Sicily, Italy), where on 2 February 2014 a rain-induced shallow landslide occurred, causing disruptions to the road network [47–49]. Figure 1 shows the location of the Municipality and the homonymous Province in the Sicily Region, along with a detail of the study area and its orthophoto. Both the territorial limits and the orthophoto are provided by the Open Data service of the Sicily Region: the first in Shapefile, the second with a Web Map Service (WMS) technology.

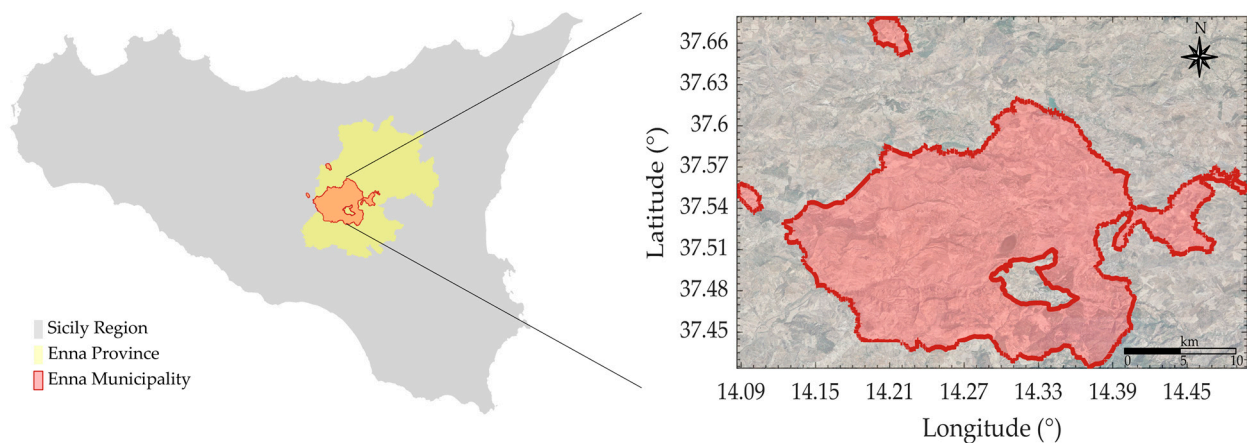


Figure 1. Geographical framework and detail of the study area.

The study area has an extent of 357 km². The Digital Terrain Model of the Sicily Region was derived through Laser Imaging Detection and Ranging (LIDAR) technology during ATA 2007–2008 flight; it deals with a medium-high-resolution DTM of cell size 2 m × 2 m. It is provided by the Web Coverage Service (WCS) of the Open Geospatial Consortium (OGC). Due to its extent, it is necessary to manage DTMs of smaller dimensions to cover the area under examination. Specifically, 20 DTMs have been used, each of a size around 40 Mb; the division of the regional DTM has been performed according to the limits of the Regional Technical Map. DTMs have been downloaded as GeoTiff and imported to MATLAB through the specific procedure reported in Table 1, obtaining the elevation matrix *E* and the MapCellReference array *R*. *E*-matrix values are shown in Figure 2a; it can be observed how elevation ranges between 230 and 990 m above sea level. As mentioned in Section 2.4.3, a common procedure for landslide susceptibility assessment is the grouping of data into parameter ranges through the MATLAB *find* function. As an example, 12 elevation classes are chosen, whose distribution is shown in Figure 2b.

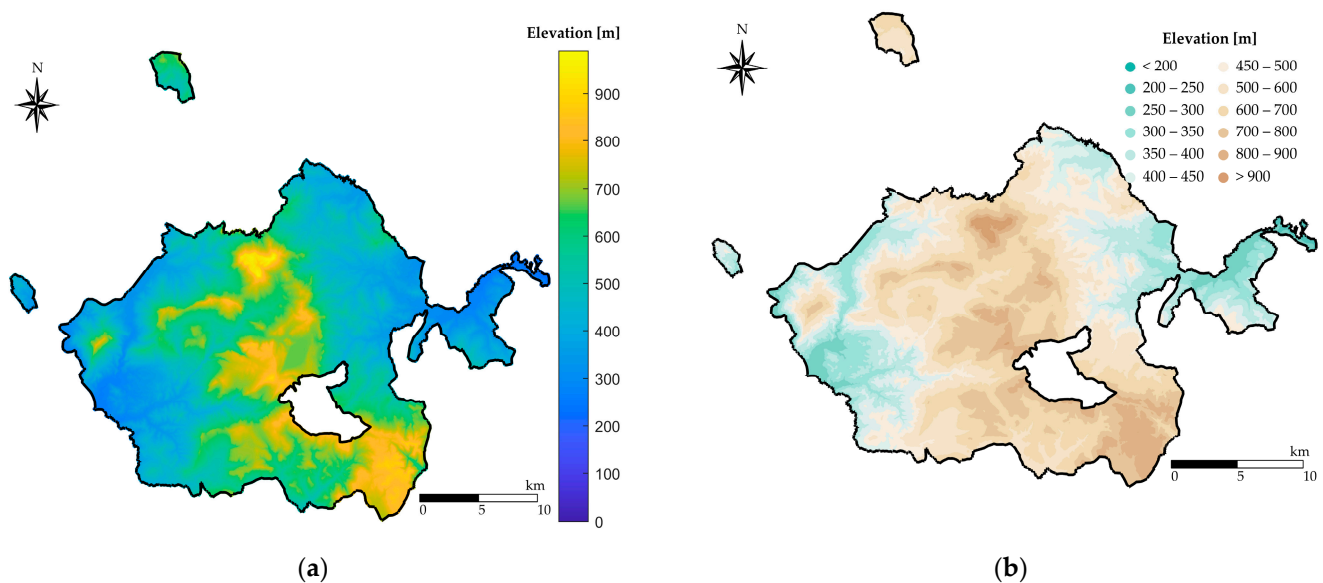


Figure 2. Elevation matrix represented in: (a) Continuous colour map; (b) Value range map.

The DTM is provided in EPSG:3004 projected coordinates (Monte Mario Italy 2); after converting the *R* array into geographic coordinates, the function *gradientm* is applied, providing the results of slope and aspect angle, respectively, shown in Figure 3a,b; even in this case, values have been grouped into classes.

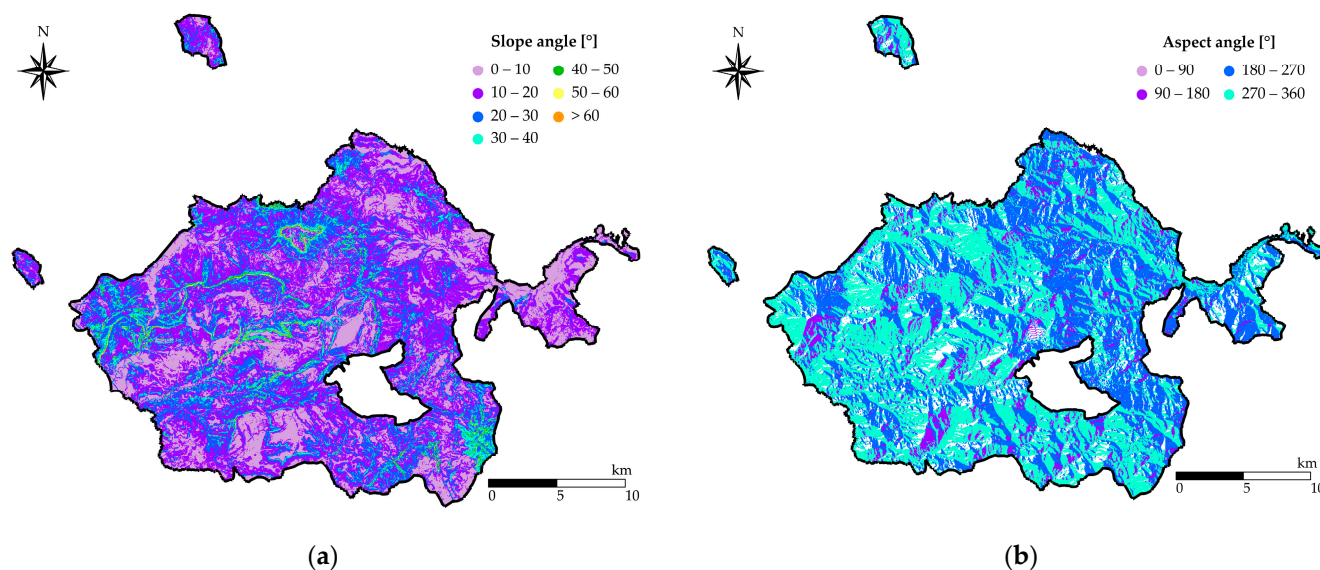


Figure 3. Morphologic parameters. (a) Slope angle; (b) Aspect angle. Both plots are range scatter plots.

The lithology of the study area is provided as a shapefile by the Open Enna database; it consists of 30 categorical lithologic units, summarised in Table 2. The methodology described in Section 2.2 is followed to obtain the field polygons plotted in Figure 4a. As discussed, a “polygon-raster” conversion is needed to assign a field parameter to each point of the reference grid; by assuming the lithologic units of the study area are grouped into 3 classes, indicated in Table 2, a class distribution is obtained using the *inpoly* function (Figure 4b).

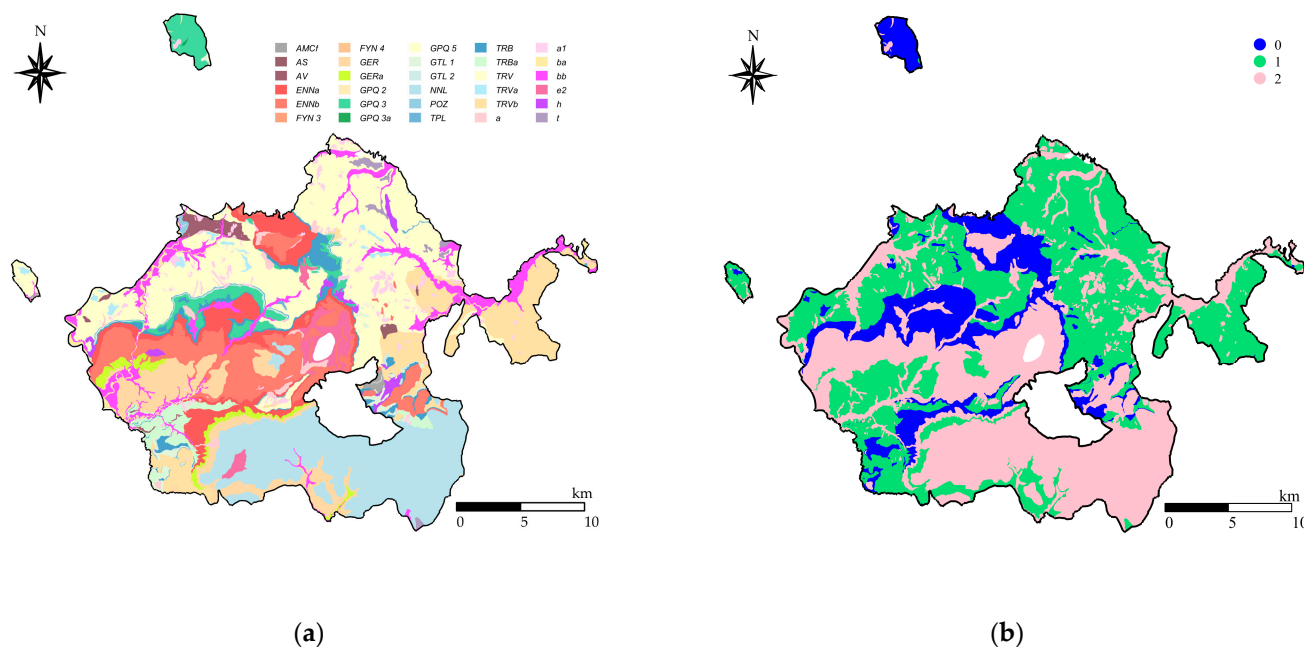


Figure 4. Lithology distribution of the study area. (a) Original distribution; (b) Representation of fields grouped according to classes assumed in Table 2: “0” refers to stone-like, “1” cohesive and “2” cohesionless soil.

Table 2. Lithology units in the study area: codes, denominations, descriptions, and classes assigned to group similar type.

Lithological Code	Denomination	Description	Class
AMCf	Centuripe formation	Blue marly clay	1
AS	Scaly clay	Scaly clay	1
AV	Variegated clay	Variegated clay	1
ENNa	Enna formation	Marl and clayey marl	0
ENNb	Enna formation	Sand and Limestone	2
FYN3	Numidian flysh	Blackish clay, brown clay and yellowish quartz sandstone	1
FYN4	Numidian flysch	Quartz, kaolinitic mudstones and silty clay	1
GER	Geracello formation	Marly clay	1
GERa	Geracello formation	Sandy clay and clayey sand	2
GPQ2	Pasquasia formation	Gypsum arenite	2
GPQ3	Pasquasia formation	Marly gypsum	0
GPQ 3a	Pasquasia formation	Gypsum	0
GPQ5	Pasquasia formation	Sandy-gypsum brownish clays	1
GTL1	Cattolica formation	Limestone	0
GTL2	Cattolica formation	Selenite	0
NNL	Lannari formation	Medium/fine-grained sand	2
POZ	Polizzi formation	Calcluties	0
TPL	Tripoli	Laminated diatomites	0
TRB	Trubi	Calcareous marl and marly limestone	0
TRBa	Trubi	Claystone breccias and brecciated clays	1
TRV	Terravecchia formation	Clayey marl and marly-silty clay	1
TRVa	Terravecchia formation	Conglomerates	0
TRVb	Terravecchia formation	Claystone breccias and brecciated clays	1
a	Colluvium deposits	Sand with many cobbles and boulders	2
a1	Landslide deposits	Heterogeneous materials	2
ba	Alluvial deposits	Gravel, sand and clayey silt	2
bb	Recent alluvial deposits	Medium-fine grained sand	2
e2	Lacustrine deposits	Sandy loam	2
h	Anthropic deposits	Gravel, sand, silt, clay	2
t	Alluvial terrace deposits	Gravel, sand, silt, clay	2

Information on land use are contained in the Corine Map provided by the Open Database of the Sicily Region as a shapefile. The procedure described in Section 2.3 is followed; the polygons' distribution is shown in Figure 5, evidencing the presence of 42 classes. In this case, no elaboration procedure for the derivation of the conditioning factors is illustrated, because it depends on the specific landslide susceptibility assessment methodology [15].

As regards rainfall, data recorded on 1 February 2014 23:00 CET by the six gauging stations illustrated in Figure 6a, provided by the Sicilian Agrometeorological Information Service (SIAS), are used. The irregular scattered data values reported in brackets have been interpolated through the *scatteredInterpolant* function, by considering the "Natural Neighbour" interpolation methodology, which is the best quality solution in MATLAB. The representation of the rainfall matrix obtained for the reference grid is shown in Figure 6b, with values grouped into six classes according to rainfall intensity.

The matrices of parameters described here have been obtained by considering four DTM resolutions: 2, 4, 8 and 16 m; each case corresponds to a different number of points in the reference grid. The time durations of each procedure with the DTM resolution and the point number are reported in Table 3 and plotted in Figure 7 against the number of points in the reference grid. Note that the rainfall value is referred to as the interpolation of a single rainfall event. Times vary according to the non-zero values of the sparse matrix.

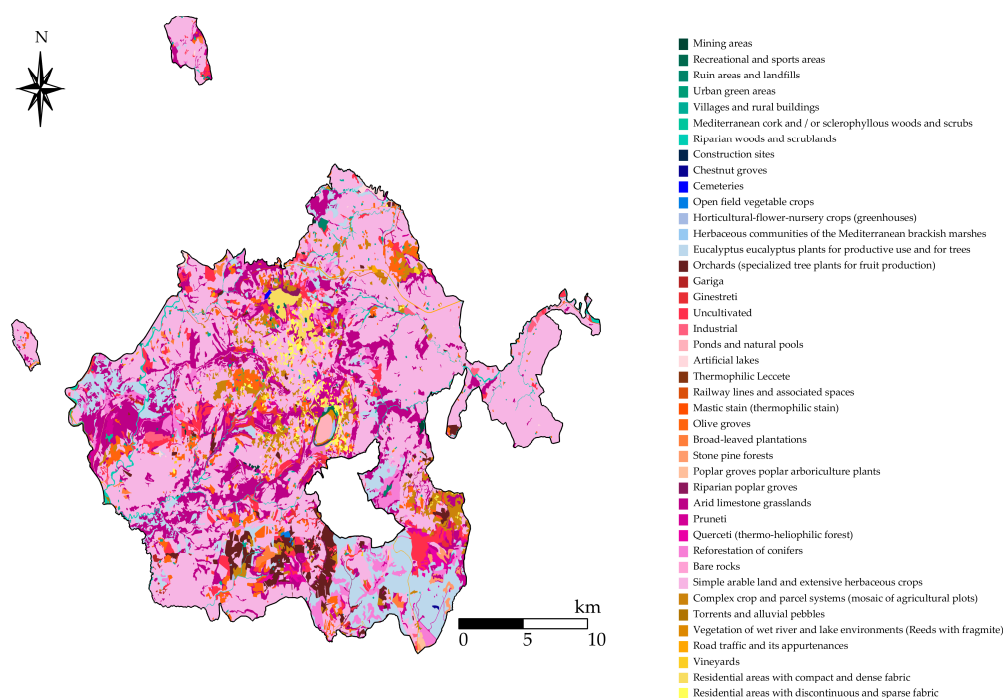


Figure 5. Land use distribution.

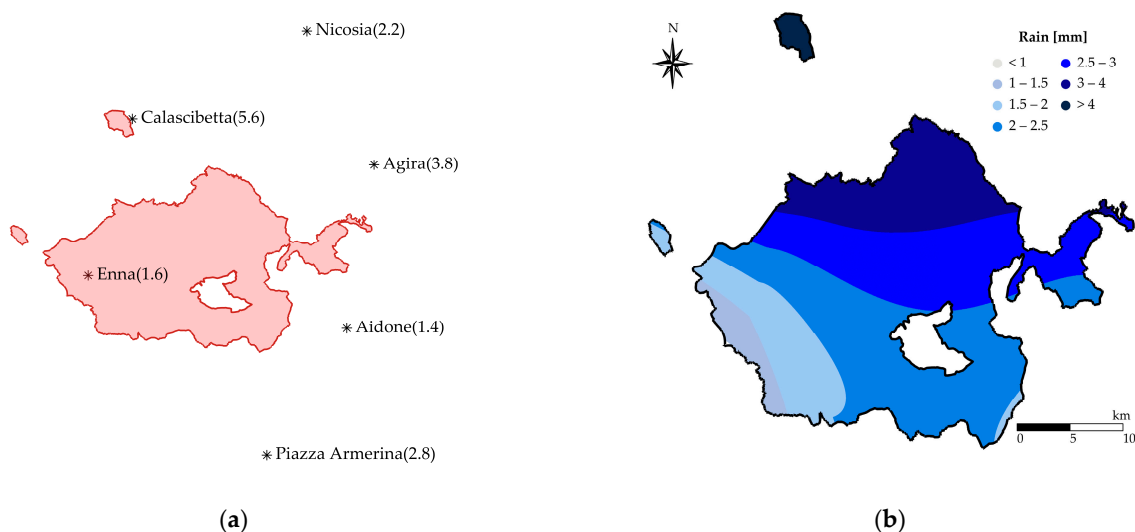


Figure 6. Rainfall data recorded on 1 February 2014 23:00 CET. (a) Distribution of the gauging stations, with the recorded values reported in brackets; (b) Map of the rainfall data interpolated through the Natural Neighbor.

Table 3. Summary of the processing times (in seconds) by changing raster resolution, related to the use of a desktop PC. equipped with Intel® Core™ i5-9600K CPU@3.70GHz, 16Gb RAM at 2133 MHz and no dedicated GPU.

Raster Samples (-)	Merging, Data Store in Cell Array and Computing of Geomorphology Parameters (s)	Clipping (s)	Polygon to Raster Conversion (<i>inpoly</i>) (s)	Rainfall Interpolation (s)
83,656,084 (2 × 2 m)	81.21	17.17	203.60	110.74
22,420,209 (4 × 4 m)	21.70	2.95	43.92	27.01
5,609,137 (8 × 8 m)	7.49	0.92	15.30	6.75
1,403,860 (16 × 16 m)	3.13	0.28	7.59	1.75

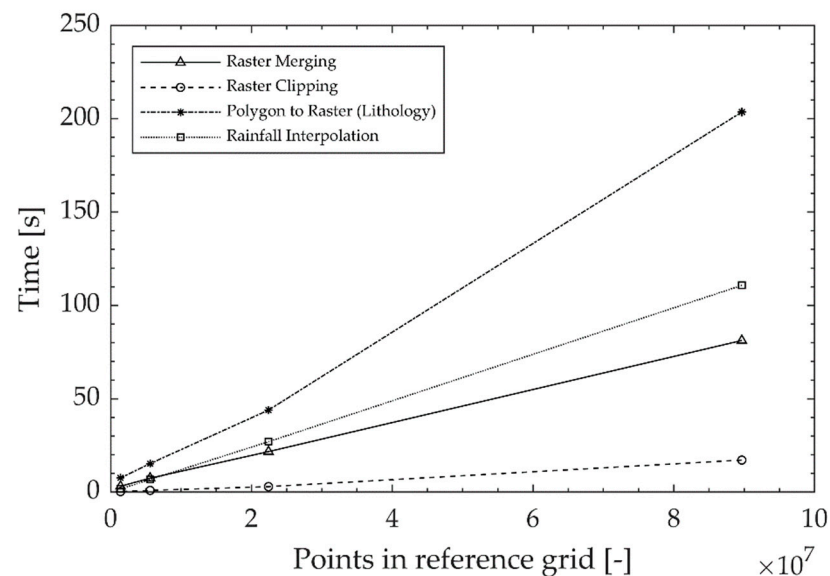


Figure 7. Time trend of different processing phases varying with raster sampling.

4. Discussion

Figures 1–6 demonstrate that, even for the solution of problems involving geodata, MATLAB may be fully applied; if GIS is defined as a tool to display geodata in a “fashionable” way [50], our plots show that MATLAB gives results similar to GIS-based elaborations, shown in most of papers about this topic [15,16,26,27,29].

Among the described procedures, the slowest one is the polygon–raster conversion and the detection of reference grid points belonging to lithology (30 fields); the raster clipping is instead the fastest operation (Figure 7). As expected, computational efficiency improves by reducing the number of points in the reference grid, with a non-linear trend. A proper selection of the raster resolution is fundamental to solving problems related to very large areas, compatible with the physical phenomenon.

Further developments regard the implementation of a fully integrated MATLAB platform for risk management, based on even complex methodologies.

Author Contributions: Conceptualization, M.P.A.G.; methodology, M.P.A.G.; software, M.P.A.G.; validation, M.P.A.G. and S.M.; formal analysis, M.P.A.G.; investigation, M.P.A.G.; resources, L.M.; data curation, M.P.A.G.; writing—original draft preparation, M.P.A.G.; writing—review and editing, M.P.A.G. and S.M.; visualization, M.P.A.G.; supervision, L.M.; project administration, L.M.; funding acquisition, L.M. All authors have read and agreed to the published version of the manuscript.

Funding: This research received no external funding.

Institutional Review Board Statement: Not applicable.

Informed Consent Statement: Not applicable.

Data Availability Statement: Not applicable.

Conflicts of Interest: The authors declare no conflict of interest.

References

1. Varnes, D.J. Slope movement types and processes. In *Landslides, Analysis and Control, Special Report 176: Transportation Research Board*; Schuster, R.L., Krizek, R.J., Eds.; National Academy of Sciences: Washington, DC, USA, 1978.
2. Haque, U.; Da Silva, P.F.; Devoli, G.; Pilz, J.; Zhao, B.; Khaloua, A.; Wilopo, W.; Andersen, P.; Lu, P.; Lee, J.; et al. The human cost of global warming: Deadly landslides and their triggers (1995–2014). *Sci. Total Environ.* **2019**, *682*, 673–684. [[CrossRef](#)] [[PubMed](#)]
3. Shano, L.; Raghuvanshi, T.K.; Meten, M. Landslide susceptibility evaluation and hazard zonation techniques—A review. *Geoenviron. Disasters* **2020**, *7*, 18. [[CrossRef](#)]
4. Roccati, A.; Paliaga, G.; Luino, F.; Faccini, F.; Turconi, L. GIS-Based Landslide Susceptibility Mapping for Land Use Planning and Risk Assessment. *Land* **2021**, *10*, 162. [[CrossRef](#)]

5. Lee, S.; Pradhan, B. Landslide hazard mapping at Selangor, Malaysia using frequency ratio and logistic regression models. *Landslides* **2007**, *4*, 33–41. [\[CrossRef\]](#)
6. Yalcin, A.; Reis, S.; Aydinoglu, A.C.; Yomralioglu, T. A GIS-based comparative study of frequency ratio, analytical hierarchy process, bivariate statistics and logistics regression methods for landslide susceptibility mapping in Trabzon, NE Turkey. *Catena* **2011**, *85*, 274–287. [\[CrossRef\]](#)
7. Felicísimo, Á.M.; Cuartero, A.; Remondo, J.; Quirós, E. Mapping landslide susceptibility with logistic regression, multiple adaptive regression splines, classification and regression trees, and maximum entropy methods: A comparative study. *Landslides* **2012**, *10*, 175–189. [\[CrossRef\]](#)
8. Li, L.; Lan, H.; Guo, C.; Zhang, Y.; Li, Q.; Wu, Y. A modified frequency ratio method for landslide susceptibility assessment. *Landslides* **2017**, *14*, 727–741. [\[CrossRef\]](#)
9. Wang, Q.; Li, W. A GIS-based comparative evaluation of analytical hierarchy process and frequency ratio models for landslide susceptibility mapping. *Phys. Geogr.* **2017**, *38*, 318–337. [\[CrossRef\]](#)
10. Mersha, T.; Meten, M. GIS-based landslide susceptibility mapping and assessment using bivariate statistical methods in Simada area, northwestern Ethiopia. *Geoenviron. Disasters* **2020**, *7*, 20. [\[CrossRef\]](#)
11. Eiras, C.G.S.; Souza, J.R.G.; Freitas, R.D.A.; Barella, C.F.; Pereira, T.M. Discriminant analysis as an efficient method for landslide susceptibility assessment in cities with the scarcity of predisposition data. *Nat. Hazards* **2021**, *107*, 1427–1442. [\[CrossRef\]](#)
12. Montrasio, L. Stability analysis of soil slip. In Proceedings of the International Conference Risk, Munich, Germany, 15–18 October 2000; Brebbia, C.A., Ed.; Wit Press, Southampton: Boston, MA, USA, 2000.
13. Goetz, J.N.; Guthrie, R.H.; Brenning, A. Integrating physical and empirical landslide susceptibility models using generalized additive models. *Geomorphology* **2011**, *129*, 376–386. [\[CrossRef\]](#)
14. Ghosh, S.; Carranza, E.J.M.; van Westen, C.J.; Jetten, V.G.; Bhattacharya, D.N. Selecting and weighting spatial predictors for empirical modeling of landslide susceptibility in the Darjeeling Himalayas (India). *Geomorphology* **2011**, *131*, 35–56. [\[CrossRef\]](#)
15. Montrasio, L.; Valentino, R.; Losi, G.L. Towards a real-time susceptibility assessment of rainfall-induced shallow landslides on a regional scale. *Nat. Hazards Earth Syst. Sci.* **2011**, *11*, 1927–1947. [\[CrossRef\]](#)
16. Montrasio, L.; Valentino, R.; Corina, A.; Rossi, L.; Rudari, R. A prototype system for space–time assessment of rainfall-induced shallow landslides in Italy. *Nat. Hazards* **2014**, *74*, 1263–1290. [\[CrossRef\]](#)
17. Formetta, G.; Capparelli, G.; Versace, P. Evaluating performance of simplified physically based models for shallow landslide susceptibility. *Hydrol. Earth Syst. Sci.* **2016**, *20*, 4585–4603. [\[CrossRef\]](#)
18. Gutiérrez-Martín, A. A GIS-physically-based emergency methodology for predicting rainfall-induced shallow landslide zonation. *Geomorphology* **2020**, *359*, 107121. [\[CrossRef\]](#)
19. Medina, V.; Hürlimann, M.; Guo, Z.; Lloret, A.; Vaunat, J. Fast physically-based model for rainfall-induced landslide susceptibility assessment at regional scale. *Catena* **2021**, *201*, 105213. [\[CrossRef\]](#)
20. Peng, L.; Niu, R.; Huang, B.; Wu, X.; Zhao, Y.; Ye, R. Landslide susceptibility mapping based on rough set theory and support vector machines: A case of the three gorges area, China. *Geomorphology* **2014**, *204*, 287–301. [\[CrossRef\]](#)
21. Arnone, E.; Francipane, A.; Scarbaci, A.; Puglisi, C.; Noto, L.V. Effect of raster resolution and polygon-conversion algorithm on landslide susceptibility mapping. *Environ. Model. Softw.* **2016**, *84*, 467–481. [\[CrossRef\]](#)
22. Ortiz, J.A.V.; Martínez-Graña, A.M. A neural network model applied to landslide susceptibility analysis (Capitanajo, Colombia). *Geomat. Nat. Hazards Risk* **2018**, *9*, 1106–1128. [\[CrossRef\]](#)
23. Chen, W.; Shahabi, H.; Shirzadi, A.; Hong, H.; Akgun, A.; Tian, Y.; Liu, J.; Zhu, A.; Li, S. Novel hybrid artificial intelligence approach of bivariate statistical-methods-based kernel logistic regression classifier for landslide susceptibility modeling. *Bull. Eng. Geol. Environ.* **2019**, *78*, 4397–4419. [\[CrossRef\]](#)
24. Bragagnolo, L.; da Silva, R.V.; Grzybowski, J.M.V. Artificial neural network ensembles applied to the mapping of landslide susceptibility. *Catena* **2020**, *184*, 104240. [\[CrossRef\]](#)
25. Sufi, F.K. AI-Landslide: Software for acquiring hidden insights from global landslide data using Artificial Intelligence. *Softw. Impacts* **2021**, *10*, 100177. [\[CrossRef\]](#)
26. Kamran, K.V.; Feizizadeh, B.; Khorrami, B.; Ebadi, Y. A comparative approach of support vector machine kernel functions for GIS-based landslide susceptibility mapping. *Appl. Geomat.* **2021**, *13*, 837–851. [\[CrossRef\]](#)
27. Ali, S.A.; Parvin, F.; Vojteková, J.; Costache, R.; Linh, N.T.T.; Pham, Q.B.; Vojtek, M.; Gigović, L.; Ahmad, A.; Ghorbani, M.A. GIS-based landslide susceptibility modeling: A comparison between fuzzy multi-criteria and machine learning algorithms. *Geosci. Front.* **2021**, *12*, 857–876. [\[CrossRef\]](#)
28. Ma, Z.; Mei, G.; Piccialli, F. Machine learning for landslides prevention: A survey. *Neural. Comput. Appl.* **2021**, *33*, 10881–10907. [\[CrossRef\]](#)
29. Pham, Q.B.; Achour, Y.; Ali, S.A.; Parvin, F.; Vojtek, M.; Vojteková, J.; Al-Ansari, N.; Achu, A.L.; Costache, R.; Khedher, K.M.; et al. A comparison among fuzzy multi-criteria decision making, bivariate, multivariate and machine learning models in landslide susceptibility mapping. *Geomat. Nat. Hazards Risk* **2021**, *12*, 1741–1777. [\[CrossRef\]](#)
30. Youssef, A.M.; Pourghasemi, H.R. Landslide susceptibility mapping using machine learning algorithms and comparison of their performance at Abha Basin, Asir Region, Saudi Arabia. *Geosci. Front.* **2021**, *12*, 639–655. [\[CrossRef\]](#)
31. Rahaman, A.; Venkatesan, M.S.; Ayyamperumal, R. GIS-based landslide susceptibility mapping method and Shannon entropy model: A case study on Sakaleshapur Taluk, Western Ghats, Karnataka, India. *Arab. J. Geosci.* **2021**, *14*, 2154. [\[CrossRef\]](#)

32. Zhao, P.; Masoumi, Z.; Kalantari, M.; Aflaki, M.; Mansourian, A. A GIS-Based Landslide Susceptibility Mapping and Variable Importance Analysis Using Artificial Intelligent Training-Based Methods. *Remote Sens.* **2022**, *14*, 211. [CrossRef]
33. Carrara, A. A multivariate model for landslide hazard evaluation. *Math. Geol.* **1983**, *15*, 403–426. [CrossRef]
34. Meijerink, A.M.J. Data acquisition and data capture through terrain mapping unit. *Int. Comput. J.* **1988**, *1*, 23–44.
35. Pike, R.J. The geometric signature: Quantifying landslide terrain types from digital elevation models. *Math. Geol.* **1988**, *20*, 491–511. [CrossRef]
36. Carrara, A.; Cardinali, M.; Detti, R.; Guzzetti, F.; Pasqui, V.; Reichenbach, P. GIS techniques and statistical models in evaluating landslide hazard. *Earth Surf. Process. Landf.* **1991**, *16*, 427–445. [CrossRef]
37. Van Westen, C.J. Application of Geographical Information System to Landslide Hazard Zonation. Ph.D. Thesis, ITC Publication, Enschede, The Netherlands, 1993.
38. Hearn, G.J.; Griffiths, J.S. Landslide hazard mapping and risk assessment. *Geol. Soc. Spec. Publ.* **2001**, *18*, 43–52. [CrossRef]
39. Lee, S.; Min, K. Statistical analysis of landslide susceptibility at Yongin, Korea. *Environ. Geol.* **2001**, *40*, 1095–1113. [CrossRef]
40. Ba, Q.; Chen, Y.; Deng, S.; Yang, J.; Li, H. A comparison of slope units and grid cells as mapping units for landslide susceptibility assessment. *Earth Sci. Inform.* **2018**, *11*, 373–388. [CrossRef]
41. Hormann, K.; Agathos, A. The point in polygon problem for arbitrary polygons. *Comput. Geom.* **2001**, *20*, 131–144. [CrossRef]
42. Kepner, J.; Kipf, A.; Engwirda, D.; Vembar, N.; Jones, M.; Milechin, L.; Gadepally, V.; Hill, C.; Kraska, T.; Arcand, W.; et al. Fast Mapping onto Census Blocks. In Proceedings of the 2020 IEEE High Performance Extreme Computing Conference, Waltham, MA, USA, 22–24 September 2020. [CrossRef]
43. Engwirda, D. Locally-Optimal Delaunay-Refinement and Optimisation-Based Mesh Generation. Ph.D. Thesis, The University of Sydney, Sydney, Australia, 2014. Available online: <http://hdl.handle.net/2123/13148> (accessed on 5 November 2021).
44. Schlinging, B.; Signell, R.; Crosby, A. Nctoolbox (2009), Github Repository. Available online: <https://github.com/nctoolbox/nctoolbox> (accessed on 10 September 2021).
45. Cheng, M.; Wang, Y.; Engel, B.; Zhang, W.; Peng, H.; Chen, X.; Xia, H. Performance Assessment of Spatial Interpolation of Precipitation for Hydrological Process Simulation in the Three Gorges Basin. *Water* **2017**, *9*, 838. [CrossRef]
46. Yoshpe, M. Distance from Points to Polyline or Polygon, MATLAB Central File Exchange. 28 January 2022. Available online: <https://www.mathworks.com/matlabcentral/fileexchange/12744-distance-from-points-to-polyline-or-polygon> (accessed on 10 January 2022).
47. Castelli, F.; Castellano, E.; Contino, F.; Lentini, V. A Web-based GIS system for landslide risk zonation: The case of Enna area (Italy). In Proceedings of the 12th International Symposium on Landslides, Napoli, Italy, 12–19 June 2016.
48. Castelli, F.; Freni, G.; Lentini, V.; Fichera, A. Modelling of a debris flow event in the Enna area for hazard assessment. In Proceedings of the 1st International Conference on the Material Point Method (MPM 2017), Delft, The Netherlands, 10–13 January 2017; Volume 175, pp. 287–292.
49. Lentini, V.; Distefano, G.; Castelli, F. Consequence analyses induced by landslides along transport infrastructures in the Enna area (South Italy). *Bull. Eng. Geol. Environ.* **2019**, *78*, 4123–4138. [CrossRef]
50. Ottens, H.F.L. GIS in Europe. In Proceedings of the II European Conference on GIS, Brussels, Belgium, 2–5 April 1991; Volume 1, pp. 1–9.